International Journal of Heat and Fluid Flow 74 (2018) 28–35

Contents lists available at ScienceDirect

International Journal of Heat and Fluid Flow

journal homepage: www.elsevier.com/locate/ijhff

Numerical investigation of bubble shape and flow filed of gas–liquid slug flow in circular microchannels

Ryo Kurimoto[a,*], Kosuke Hayashi[b], Hisato Minagawa[a], Akio Tomiyama[b]

[a] Department of Mechanical Systems Engineering, University of Shiga Prefecture, 2500, Hassaka, Hikone, Shiga, Japan
[b] Graduate School of Engineering, Kobe University, 1-1, Rokkodai, Nada, Kobe, Japan

ARTICLE INFO

Keywords:
Slug flow
Circular microchannel
Numerical simulation
Volume of fluid method

ABSTRACT

Numerical simulations of gas–liquid slug flows (also known as Taylor flows) in circular microchannels are carried out using an interface tracking method based on the volume of fluid method to investigate effects of relevant dimensionless numbers on the bubble shape and the flow structure inside and outside a bubble. Uniform slug flows are dealt with, and therefore, the motion of a single unit cell consisting of a Taylor bubble and a liquid slug is predicted. Adaptive computational cells are used to capture the thin liquid film between a bubble and the channel wall. The numerical conditions are the same as those in experiments in our previous study, i.e. two channel diameters and three liquids of different viscosities are used. The conclusions obtained are as follows: (1) the interface tracking simulation can give good predictions of the bubble shape and the relationship between the void fraction and the gas volumetric flow ratio, (2) the radius of curvature at the bubble nose can be well correlated in terms of the capillary number, whereas that at the bubble tail depends not only on the capillary number but also on the Weber number, and (3) the minimum liquid film thickness appearing in the tail region of a bubble, which is thinner than the uniform liquid film in the cylindrical bubble body region in all the numerical conditions, can be correlated in terms of the capillary number as well as the uniform liquid film thickness in the cylindrical bubble body region.

1. Introduction

Gas–liquid two-phase flows have been used in various microdevices, e.g. microreactors, heat exchangers and so on. Slug flow (also known as Taylor flow) is one of the typical flow patterns in gas–liquid two-phase flows in circular micorchannels (Triplett et al., 1999; Kawahara et al., 2002; Serizawa et al., 2002; Chung and Kawaji, 2004; Saisorn and Wongwises, 2008; Sur and Liu, 2012). Many studies on slug flows in circular microchannels, therefore, have been carried out.

The knowledge of bubble shape and flow field in a slug flow in a microchannel is of great importance in design and development of the microdevices since heat and mass transfer in the liquid and gas phases and channel wall are strongly affected by them. In particular, flow fields around the nose and tail of a bubble, their shapes and the liquid film thickness are primal factors governing the heat and mass transfer. Therefore numerical simulations of gas–liquid slug flows in microchannels have been carried out to obtain detailed information on bubble shapes and flow field. Zhang and Li (2016) and Rocha et al. (2017) carried out numerical simulations of gas–liquid slug flows in circular microchannels. A typical bubble shape and the flow field about the bubble obtained in their numerical simulations are schematically shown in Fig. 1, in which a large circulation is formed in the liquid slug and three circulations are formed in the bubble. The numerical conditions, e.g. the Reynolds number and the gas volume fraction, affected the flow field in the liquid slug and the size of the small circulations inside the bubble, and the bubble nose and tail shapes depended on the structure of the flow fields. Although these studies revealed some characteristics of the flow field and bubble shape, their details, e.g. the dependences of the size of circulations and the curvatures of the nose and tail on relevant flow parameters, are not sufficiently understood.

Asadolahi et al. (2012) and Langewisch and Buongiorno (2015) numerically investigated the applicability of available liquid film thickness models. Asadolahi et al. (2012) compared their numerical data of the liquid film thickness with a model proposed by Aussillous and Quéré (2000). The comparisons showed that the model is inaccurate due to neglect of the inertia effect on the liquid film thickness. Langewisch and Buongiorno (2015) compared their numerical data with the liquid film thickness model proposed by Han and Shikazono (2009), which accounts for the inertia effect, and their model. Although both models gave reasonable evaluations of the liquid

* Corresponding author.
E-mail address: kurimoto.r@mech.usp.ac.jp (R. Kurimoto).

https://doi.org/10.1016/j.ijheatfluidflow.2018.09.008
Received 23 May 2018; Received in revised form 27 August 2018; Accepted 15 September 2018

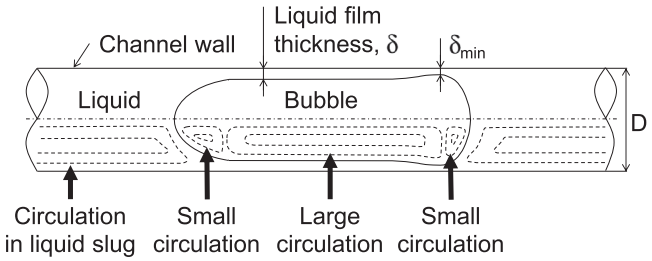

Fig. 1. Typical bubble shape and flow field of slug flow in circular microchannel
(Dotted lines represent streamlines).

film thickness, Langewisch and Buongiorno's model was more reliable.

The liquid film thickness is uniform in the cylindrical body region of a bubble, whereas it is non-uniform in the nose and tail regions and tends to take the minimum value, δ_{min}, in the tail region (Fig. 1). Although Magnini and Thome (2016) pointed out that sudden flow variation in the tail region is the cause of the minimum liquid film thickness, we have no correlations for evaluating δ_{min}.

Numerical simulations of slug flows in circular microchannels were carried out using an interface tracking method based on the volume of fluid method in this study to investigate the relationship between the bubble shape and the flow field. The numerical conditions were the same as those in experiments in our previous paper (Kurimoto et al., 2017). In the experiments, the slug flows were uniform. Since the characteristics of the uniform slug flow are governed by the dynamics of a single slug unit consisting of a liquid slug and a Taylor bubble, we focused on the single slug unit in the present numerical simulations. As is well known, the liquid film of a slug flow is very thin (Bretherton, 1961; Aussillous and Quéré, 2000; Han and Shikazono, 2009; Langewisch and Buongiorno, 2015). Computational cells were therefore adaptively assigned in the vicinity of the interface to resolve the very thin liquid films. After validating the numerical method, the effects of relevant dimensionless groups, i.e. the Reynolds, Weber and capillary numbers, on the bubble shape and the flow field were discussed.

2. Numerical method and conditions

2.1. Interface tracking method

The continuity and momentum equations for two incompressible Newtonian fluids based on the one-fluid formulation are given by

$$\nabla \cdot V = 0 \tag{1}$$

$$\frac{\partial V}{\partial t} + V \cdot \nabla V = -\frac{1}{\rho}\nabla P + \frac{1}{\rho}\nabla \cdot \mu[\nabla V + (\nabla V)^T] + \frac{1}{\rho}\sigma\kappa n\delta \tag{2}$$

where $\boldsymbol{V}$ is the velocity, t the time, ρ the density, P the pressure, μ the viscosity, σ the surface tension, κ the mean interface curvature, $\boldsymbol{n}$ the unit normal to the interface, δ the delta function which is non-zero only at the interface, and the superscript T denotes the transpose. The density is given by

$$\rho = (1 - F)\rho_G + F\rho_L \tag{3}$$

where F is the cell-averaged volume fraction of the liquid phase, and the subscripts G and L denote the gas and liquid phases, respectively. The following harmonic mean of the viscosity is used to correctly deal with the continuity of the viscous stresses (Tryggvason et al., 2011):

$$\frac{1}{\mu} = \frac{1 - F}{\mu_G} + \frac{F}{\mu_L} \tag{4}$$

The mean curvature is evaluated by using the height function technique (Cummins et al., 2005). The advection and diffusion terms are discretized by using the CIP (cubic interpolated propagation) scheme (Takewaki and Yabe, 1987) and the second-order centered-difference scheme, respectively. The ghost fluid method (Kang et al., 2000) is adopted to the surface tension force, i.e. the pressure jump due to the surface tension force is accounted for in the discretized pressure gradient.

The computational cell is filled with the liquid phase when $F = 1$, and with the gas phase when $F = 0$. A cell with $0 < F < 1$ contains an interface. The interface motion is calculated by solving the following advection equation of F:

$$\frac{\partial F}{\partial t} + \nabla \cdot FV = F\nabla \cdot V \tag{5}$$

This equation is solved using a combination of the NSS (non-uniform subcell scheme) (Hayashi et al., 2006) and the EI-LE (Eulerian Implicit-Lagragian Explicit) scheme (Aulisa et al., 2003). The right hand side of the above equation, $F\nabla\cdot\boldsymbol{V}$, which is called the divergence correction term, is introduced to conserve the fluid volume (Rider and Kothe, 1998). Since a local level set function is computed in the interface cell in the NSS, it can be used in the ghost fluid method for the surface tension force.

2.2. Computational domain and numerical condition

The computational domain is shown in Fig. 2. The two-dimensional (r, z) cylindrical coordinates were used, and the boundary at $r = 0$ was the axis of symmetry. The dimensions of the domain in the r and z directions were $0.5D$ and L, respectively, where D is the channel diameter. The boundary of $r = 0.5D$ was the channel wall. An instantaneous bubble velocity with an opposite sign $-u_G(t)$ was imposed on the wall and the instantaneous acceleration of the bubble with the opposite sign was added to Eq. (2) to fix the bubble position (Wang et al., 2008). The boundaries at $z = 0$ and L were periodic. A constant pressure gradient dP/dz was imposed between $z = 0$ and L to generate a flow in the z-direction. The initial bubble shape was composed of a cylindrical section with two hemispheres. The radius of the initial bubble was $0.425D$. The initial bubble length was determined for L and the void fraction α. The measured data obtained in our previous study (Kurimoto et al., 2017) were used for dP/dz, L and α. In order to accurately capture the liquid film between a bubble and the wall, adaptive computational cells were assigned in the vicinity of the interface (Fig. 3). The computational domain was initially divided into uniform cells, which were the coarsest cells of the size h and are referred to as the base cells. Finer cells were embedded into the base cells by a quadtree manner and the finest refinement level, l, was five, i.e. $l = 0$ for the base cells and the size of the finest cell was $h/2^4$. When the magnitude of the local level set function at a vertex of a base cell was smaller than 1.5 h, $2^4 \times 2^4$ cells at $l = 5$ were embedded into the base cell. Base cells neighboring to the cells of $l = 5$ were $l = 4$, i.e. $2^3 \times 2^3$ cells of the size $h/2^3$ were embedded into the base cells. Fine cells of $l = 1$–3 were set in the same manner. The minimum and maximum sizes of the computational cell were $0.5D/128$ and $0.5D/8$, respectively. As a result, the number of cells assigned to liquid film was at least 7 cells in all the numerical conditions. The grid convergence was examined for the air-water system (Case b1-1 in Table 2). The minimum and maximum sizes of the computational cell in the examination were varied up to $0.5D/256$ and $0.5D/16$, respectively, while the domain size was fixed. The changes in the bubble velocity and the liquid film thickness with the increase in the spatial resolution were less than 0.7 and 3.6%, respectively.

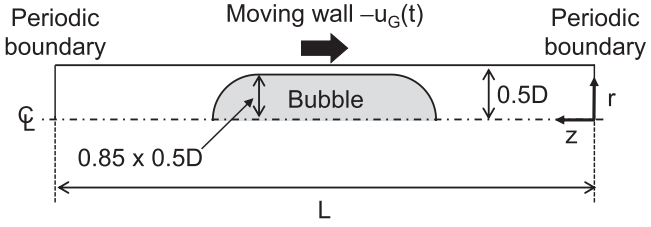

Fig. 2. Computational domain and initial bubble shape.